Defects in Nematics

1. Introduction

2. Applications

(a) Natural System

- Chiral Nematics

(b) Industrial System

Carbonaceous Mesophases (Discotic Nematics)

(c) Research System

Monomeric & Polymeric Rod-Like Nematics

Theory and governing Equations

- Director **n** is the average orientation of the unit normals **u** of an ensemble of disc like molecules

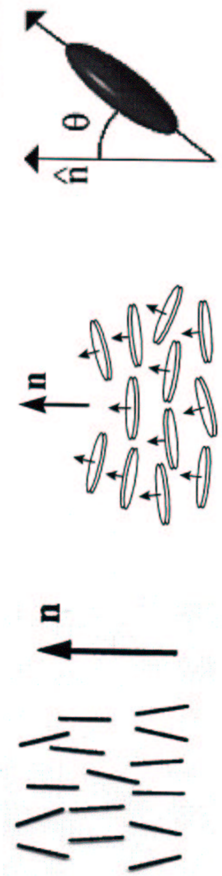

(a) (b) (c)

$$S = \left\langle \frac{3}{2}\cos^2\theta - \frac{1}{2} \right\rangle$$

Defects

$$F_d = \frac{K}{2}(\nabla \underline{n})^2 \longrightarrow \nabla^2 \underline{n} = 0$$

Singular Solutions to $\nabla^2 \underline{n} = 0$

Defects: { dimension, charge, sign }

dimension: 0 , 1 , 2

Sign: ±

Strength:

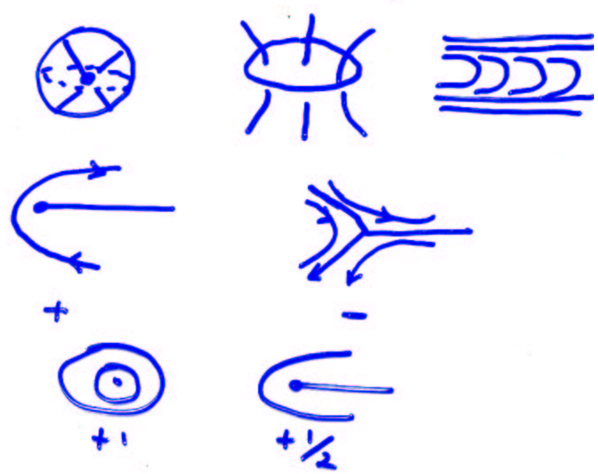

Point Defects

$$\delta \int dv F = 0; \qquad 2F = K\left((\nabla . \mathbf{n})^2 + (\nabla \times \mathbf{n})^2\right)$$

$$n = n(\phi, \theta); \qquad \phi = \phi(\alpha); \qquad \theta = \theta(\delta)$$

$$\phi = \pm\alpha + C; \qquad \tan\frac{\theta}{2} = \left(\tan\frac{\delta}{2}\right)^{|s|}$$

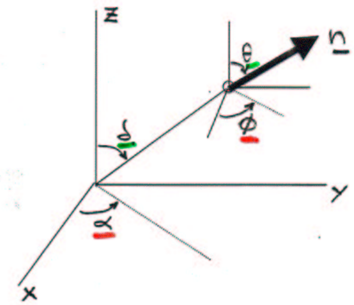

Hedgehog Point Defect :S=+1

$$\phi = +\alpha; \qquad \theta = \delta$$

$$E = 8\pi K R$$

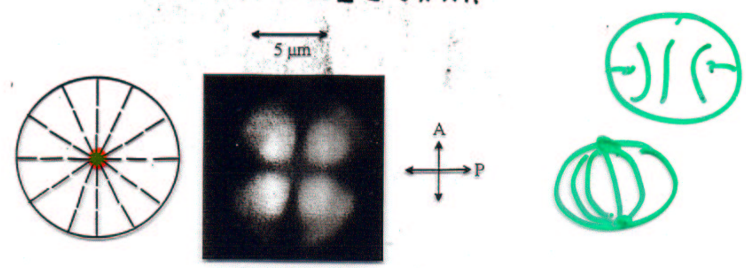

Line Defects : Disclinations

$$n_x = \cos\theta; \quad n_y = \sin\theta; \quad n_z = 0$$

$$2f = K(\nabla\theta)^2 \Rightarrow \underline{\nabla^2\theta = 0}$$

$$\theta = S\alpha + c; \qquad S = \pm 1/2, \pm 1$$

$E = KS^2 \ln\left(\frac{R}{r_c}\right)$

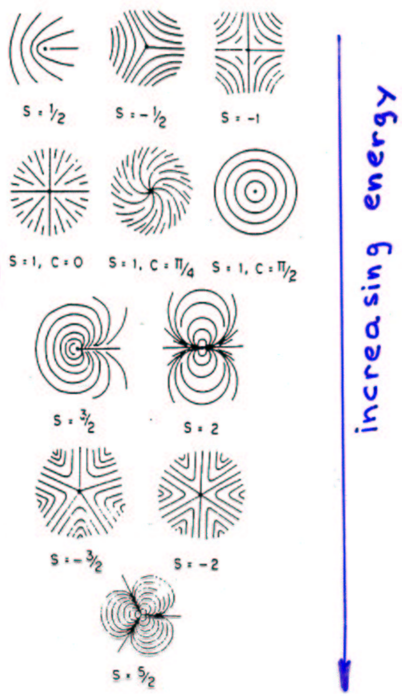

$E \propto S^2$

Defect- Defect Interaction

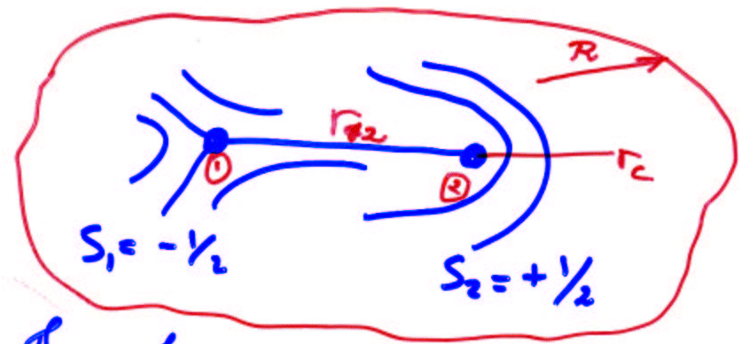

$$f_e = f_c + \pi K (s_1 + s_2)^2 \ln\left(\frac{R}{r_c}\right) - 2\pi K s_1 s_2 \ln\left(\frac{r_{12}}{2r_c}\right)$$

when $r_c << r_{12} < R$

$$F_{12} = 2\pi K \frac{S_1 S_2}{r_{12}}; \quad r_{12} >> r_c$$

Inversion Walls

-Non-singular 2D defects

Orienting field : H (magnetic or extensional flow)

$$2f = K\left((\nabla . \mathbf{n})^2 + (\nabla \times \mathbf{n})^2\right) - \chi_a (\mathbf{H}.\mathbf{n})^2$$

$$x = \pm\xi \ln(\tan\theta/2); \quad \xi = \frac{1}{H}\left(\frac{K}{\chi_a}\right)^{1/2}$$

Surface Tension $\sigma = 2\ K/\xi$

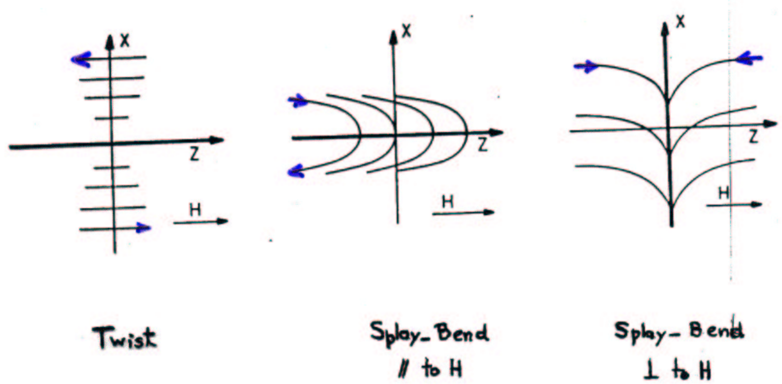

Linear Stability Analysis of Splay-Bend Walls

In plane Perturbation : $\psi(x,z,t)$ Out-of-plane Perturbation : $\xi\ (x,z,t)$

$n_x = \sin\theta + \psi \cos\theta, \quad n_y = \xi, \quad n_z = \cos\theta - \psi \sin\theta$

Solution to Autonomous PDE $\xi = \exp(st)\, \phi\ (x,z)$

Instability Threshold ($\sigma > 0$): $\pi^2\left(1 - \frac{K_{22}}{K_{33}}\right) \geq 1 + \frac{\pi^2}{4}\left(1 + 3\frac{K_{11}}{K_{33}}\right)\frac{d^2}{L^2}$

$d = \frac{1}{H}\sqrt{\frac{K}{\chi_a}}$ Perturbation wave-length : $L = \lambda$

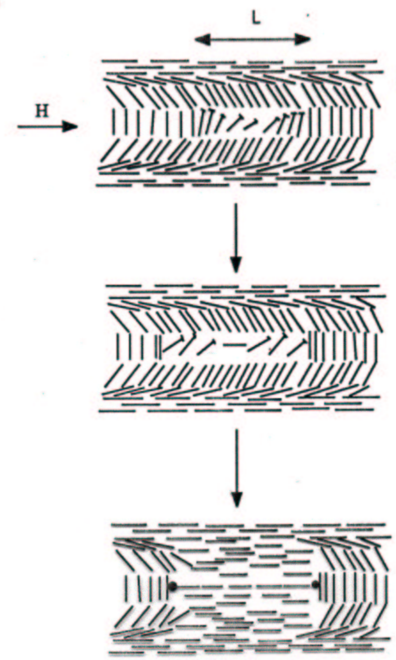

Configurational Forces

Forces acting on defects =Peach-Koehler Force

$$F = \oint \mathbf{k}.\mathbf{T}dl = \oint \mathbf{k}.\left(-p\mathbf{I} - \frac{\partial f}{\partial \nabla \mathbf{n}}.(\nabla \mathbf{n})^T\right)dl$$

Elastic stress Tensor

(a) Line-Line Force

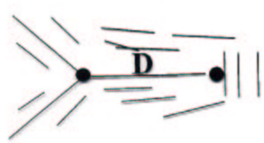

$$F = \frac{2\pi K S_1 S_2}{D}$$

←+ +→

+→ ←−

(b) Loop Tension

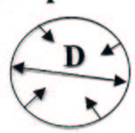

$$T(force/length) = K/\pi D$$

(c) Line-Wall Interaction

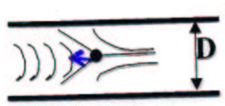

$$F = \frac{2K}{D}$$

Defect Line Energies

(energy/ℓ) $$\mathcal{F}_\ell = \underbrace{\pi r_c^2 \mathcal{E}_c}_{\text{core}} + \underbrace{\pi K S^2 \ln\left(\frac{R}{r_c}\right)}_{\text{long range}}$$

$$\frac{d\mathcal{F}_\ell}{dr_c} = 0 \rightarrow \mathcal{E}_c = \frac{KS^2}{r_c^2} \sim 10^{-7}\frac{erg}{cc}$$

$$\mathcal{F}_\ell = KS^2\left[1 + \ln\left(\frac{R}{r_c}\right)\right]$$

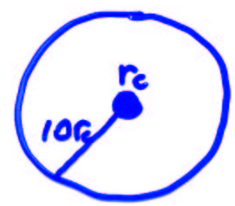

$\mathcal{F}_c \sim \mathcal{F}_{LR}$

$R \sim 10 r_c$

Structure of Disclination Line Cores

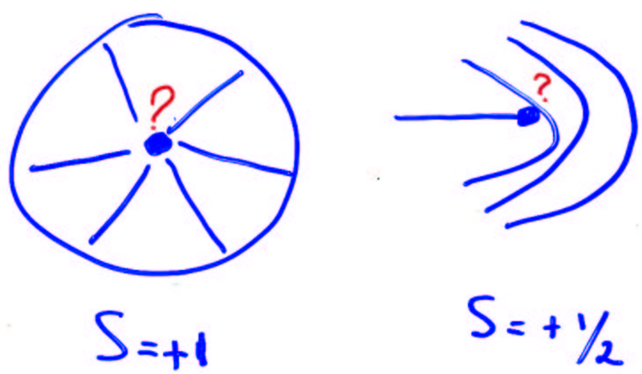

$$\underline{\underline{Q}} = \mu_n \underline{n}\,\underline{n} + \mu_m \underline{m}\,\underline{m} + \mu_\ell \underline{\ell}\,\underline{\ell}$$

$$\mu_i \overset{?}{=} \mu_i(r)$$

Theory and governing Equations

Short Range (Homogeneous) Energy Contribution:

$$F^h = \frac{1}{2}A(\mathbf{Q}:\mathbf{Q}) + \frac{1}{3}B(\mathbf{Q}:(\mathbf{Q}\cdot\mathbf{Q})) + \frac{1}{4}C\,tr(\mathbf{Q}:\mathbf{Q})^2$$

Long Range (Non-Homogeneous) Energy Contribution:

$$F^e = \frac{1}{2}L_1(\nabla\mathbf{Q}):(\nabla\mathbf{Q})^T + \frac{1}{2}L_2(\nabla\cdot\mathbf{Q})\cdot(\nabla\cdot\mathbf{Q}) + \frac{1}{2}L_3\mathbf{Q}:(\nabla\mathbf{Q}:\nabla\mathbf{Q})$$

Result & Discussion

- Analysis of Defects (Mainly +1)
  - ✓ Plots showing the variation of the three eigen values across the fiber diameter for PR and PP textures

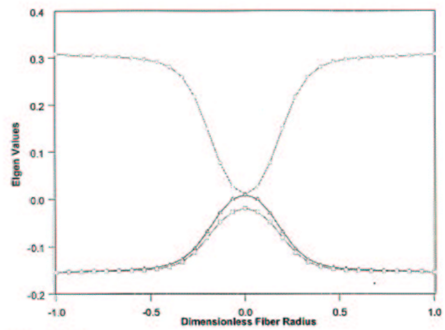

U=2.9

L_2 = -0.5

$\frac{H}{\xi} = 24.5$

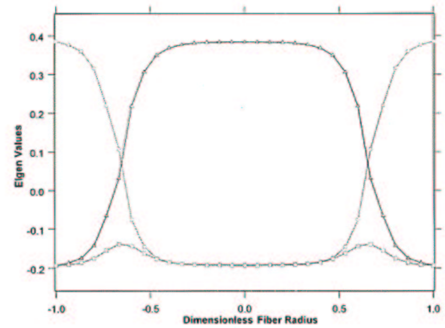

U=3.30

L_2 = -0.5

$\frac{H}{\xi} = 17.3$

Result & Discussion

- Biaxial Torus around the +1 defect
  - ✓ β^2 is a measure of the degree of biaxiality

$$\beta^2 = 1 - 6\frac{(\mathrm{tr}\,\mathbf{Q}^3)^2}{(\mathrm{tr}\,\mathbf{Q}^2)^3}$$

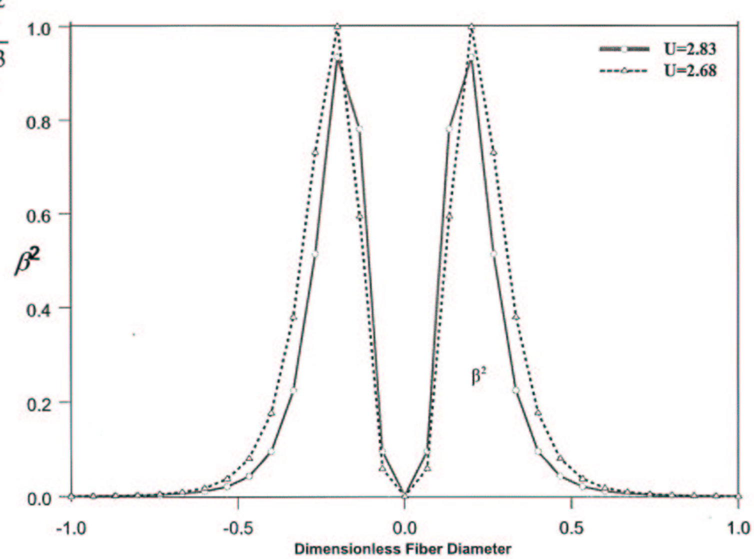

Application # 1

Chiral Nematics

5

Bouligand (1960s →); Neville (1993)

Review of experimental situations

Arced patterns in invertebrates

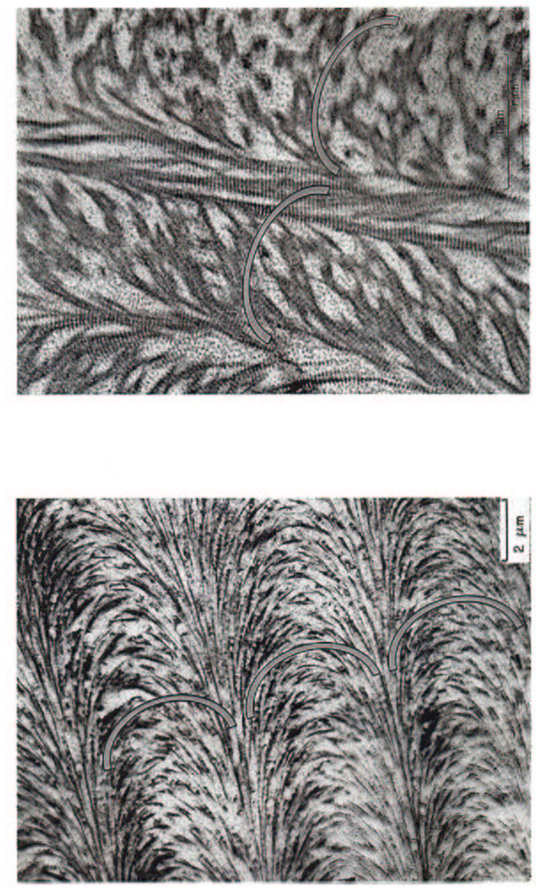

Crab cuticle

Marine Gastropod

Origin of the arced patterns

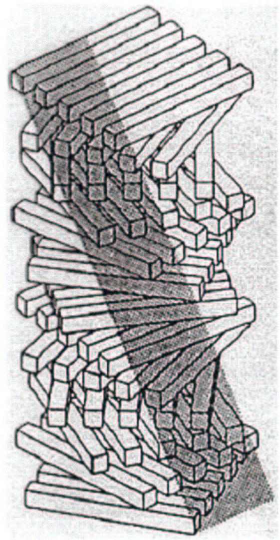

Twisted plywood-like structure

Arced patterns observed in bio-composites

7

Review of experimental situations

Arced patterns in vertebrates

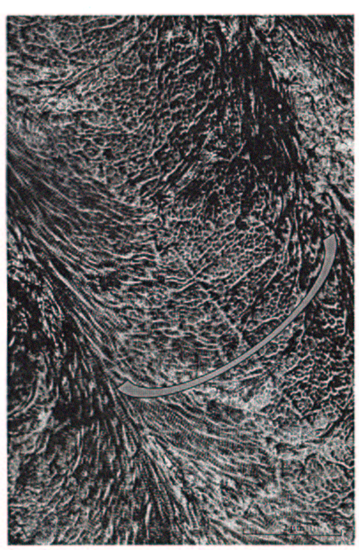

Human bone

Mantis egg case

5

6

Review of experimental situations

Arced patterns in plants

Stone cell of a pear

Why and how Monodomains?

Neville Hypothesis:

(1) Monodomain

(substrate = constraining layer

(2)

Our hypothesis: Not possible

(3)

Chiral nematic liquid crystals exhibit helically twisted structures that are similar to the one of bio-composites

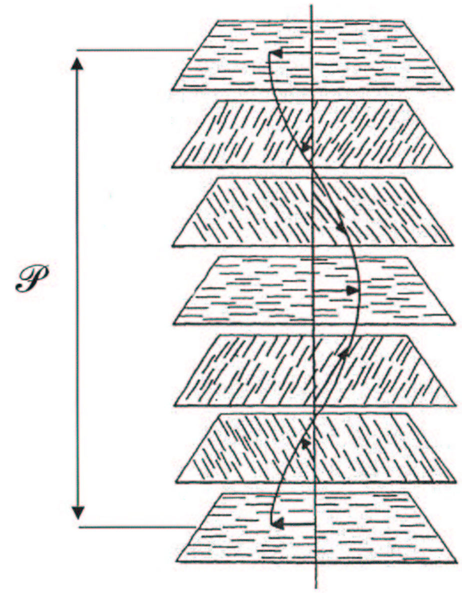

$\mathscr{P}$ = Pitch

Distance over which the molecular orientation rotates by 2π radians

11

The formation of bio-composite microstructures is investigated using a model based on the Landau-de Gennes free-energy

$$f = f_s + f_l$$

$$f_s = \frac{1}{2}\left(1-\frac{U}{3}\right)tr(\boldsymbol{Q}^2) - \frac{U}{3}tr(\boldsymbol{Q}^3) + \frac{U}{4}[tr(\boldsymbol{Q}^2)]^2$$

$$f_l = \frac{1}{2}\left\{\left(\left(\frac{\xi}{\mathscr{H}}\right)(\nabla\times\boldsymbol{Q}) + 4\pi\left(\frac{\xi}{\mathscr{P}}\right)\boldsymbol{Q}\right)^2 + \upsilon\left(\left(\frac{\xi}{\mathscr{H}}\right)(\nabla\cdot\boldsymbol{Q})\right)^2\right\}$$

U : Reduced concentration

υ : Ratio of elastic moduli

12

Dimensionless parameters of the model

$$\left(\frac{\xi}{\mathscr{H}}\right) = \frac{\text{Internal length scale}}{\text{Geometric length scale}}$$

$\left(\frac{\xi}{\mathscr{H}}\right) \to 0 \Leftrightarrow$ Microstructure driven by short - range elasticity

$\left(\frac{\xi}{\mathscr{H}}\right) \to \infty \Leftrightarrow$ Microstructure driven by long - range elasticity

$$\left(\frac{\xi}{\mathscr{P}}\right) = \frac{\text{Internal length scale}}{\text{Pitch length scale}}$$

$\left(\frac{\xi}{\mathscr{P}}\right) = 0 \Leftrightarrow$ Achiral material

$\left(\frac{\xi}{\mathscr{P}}\right) \neq 0 \Leftrightarrow$ Chiral material

13

Periodic boundary conditions are assumed in the x-direction to avoid lateral effects

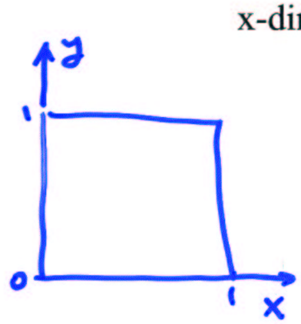

$$\boldsymbol{Q}(x=0) = \boldsymbol{Q}(x=1)$$

$$\left.\frac{\partial \boldsymbol{Q}}{\partial x}\right|_{x=0} = \left.\frac{\partial \boldsymbol{Q}}{\partial x}\right|_{x=1}$$

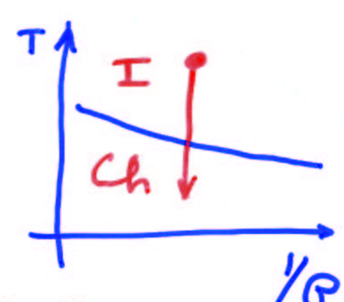

The upper side of the computational domain is assumed to be isotropic

The uniaxial director $\boldsymbol{n}$ describe a fixed planar anchoring at the lower side boundary

18

Evolution of the uniaxial and biaxial order parameters

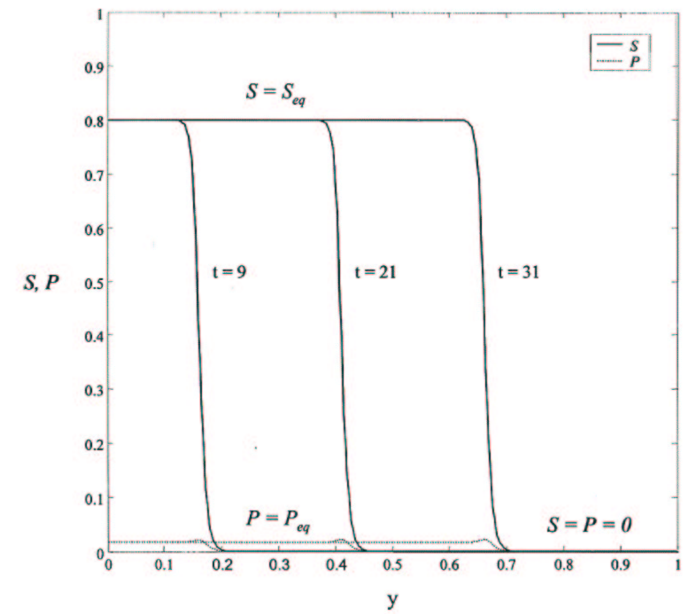

23

Dynamics of the chiral nematic-isotropic interface in the uniaxial approximation

$$S(y,t) = S(y - Vt) = S(z) \qquad S(z) = \frac{S_3}{2}\left\{1 - \tanh\left[\frac{z}{w_0}\right]\right\}$$

$$w_0 = \left(\frac{\xi}{H}\right)\frac{2}{S_3}\sqrt{\frac{3}{U}} \qquad S_3 = \frac{1}{4} + \frac{1}{4}\left(9 - \frac{24}{U} - \frac{96}{U}\pi^2\left(\frac{\xi}{P}\right)^2\right)^{1/2}$$

$$V = \left(\frac{\xi}{H}\right)\sqrt{\frac{U}{3}}\left[-\frac{1}{4} + \frac{3}{4}\left(9 - \frac{24}{U} - \frac{96}{U}\pi^2\left(\frac{\xi}{P}\right)^2\right)^{1/2}\right]$$

$$V = V\left(\frac{\xi}{H}, U, \frac{\xi}{P}\right)$$

24

The cross-sectional view of the microstructure exhibit typical series of nested arced patterns

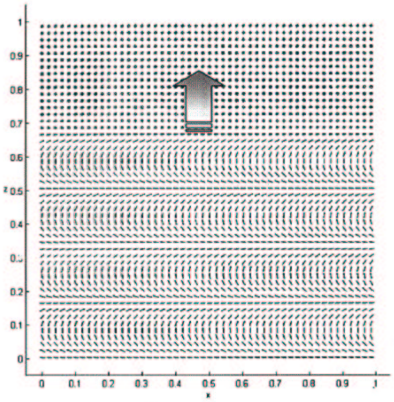

$U = 6$

$\upsilon = 1$

$\frac{\xi}{\mathscr{H}} = 0.01$

$\frac{\xi}{\mathscr{P}} = 0.01$

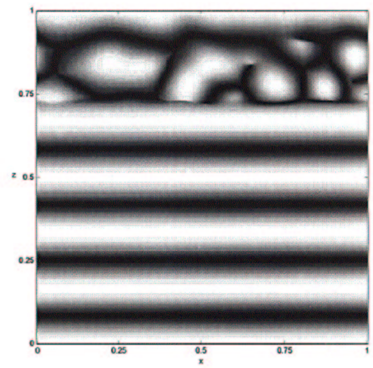

$t = 9$ $t = 9$

The polarized light intensity plot shows the commonly observed periodic extinction of light

22

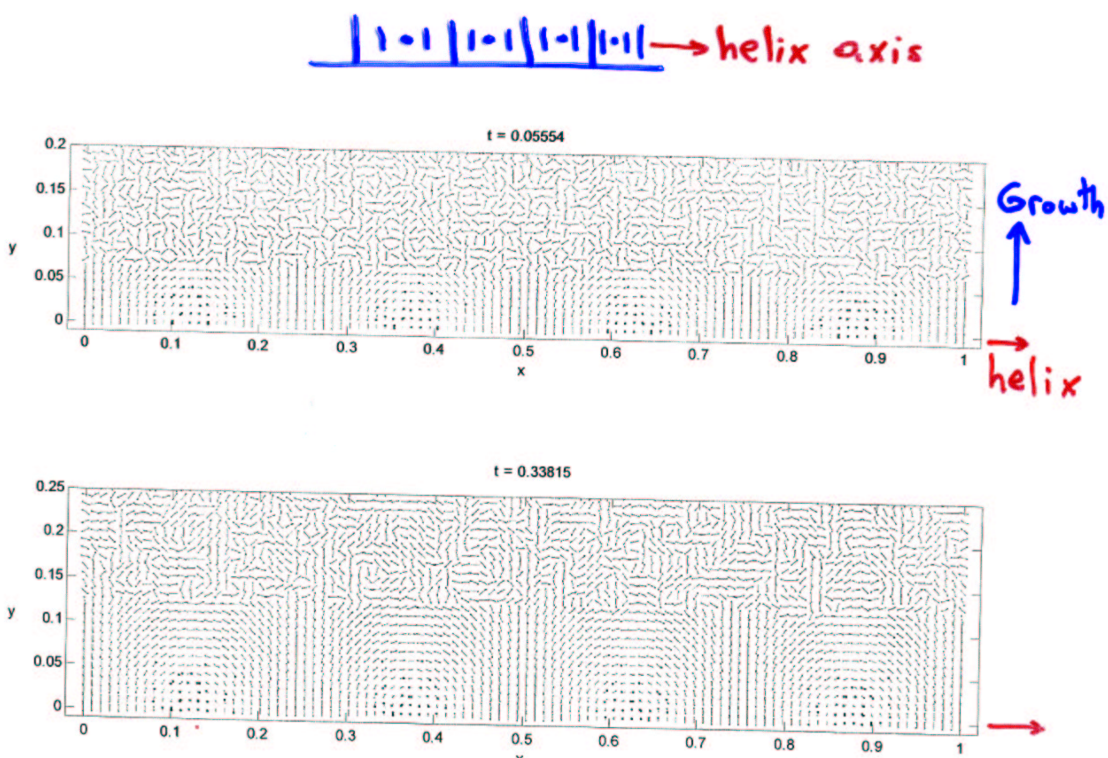

28

Helix axis normal to the front - unstable growing mode

$U = 6$

$\upsilon = 1$

$\frac{\xi}{\mathscr{H}} = 0.01$

$\frac{\xi}{\mathscr{P}} = 0.01$

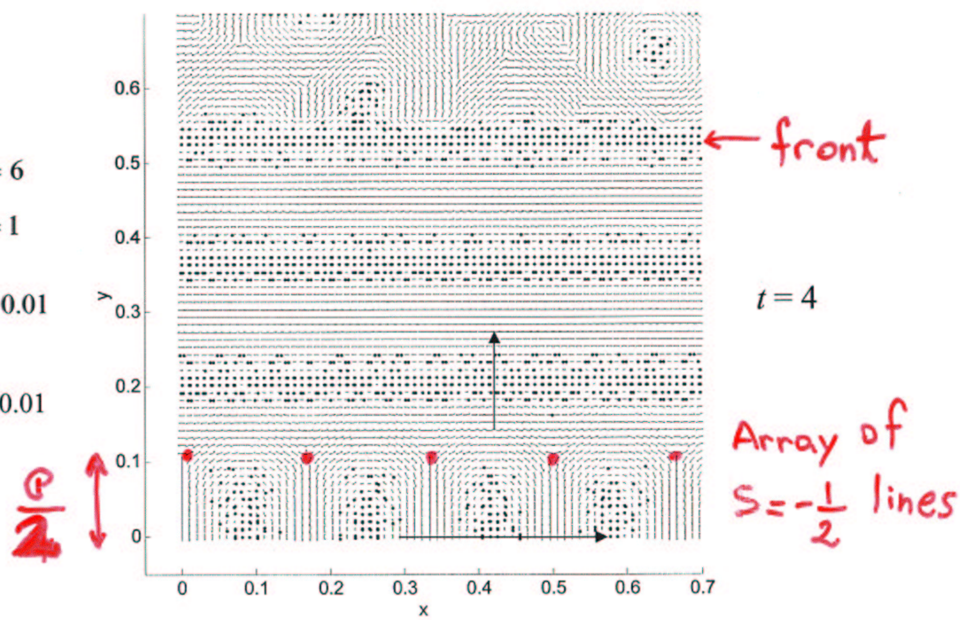

Director field showing a planar reorientation through a defect nucleation

33

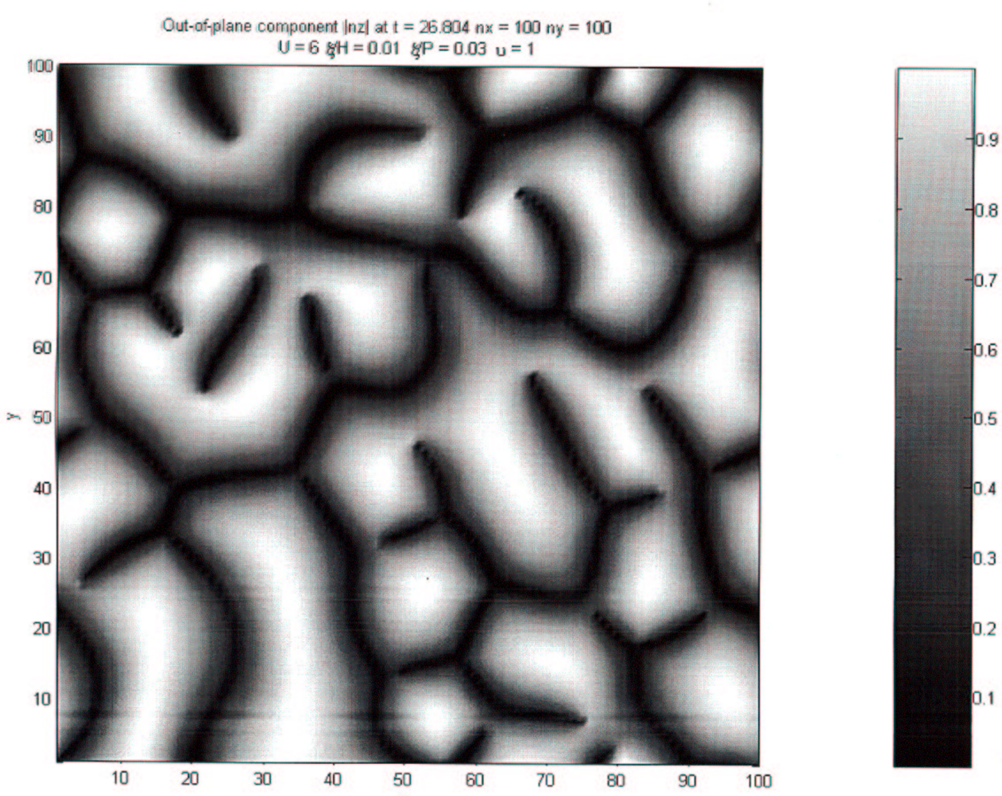

46

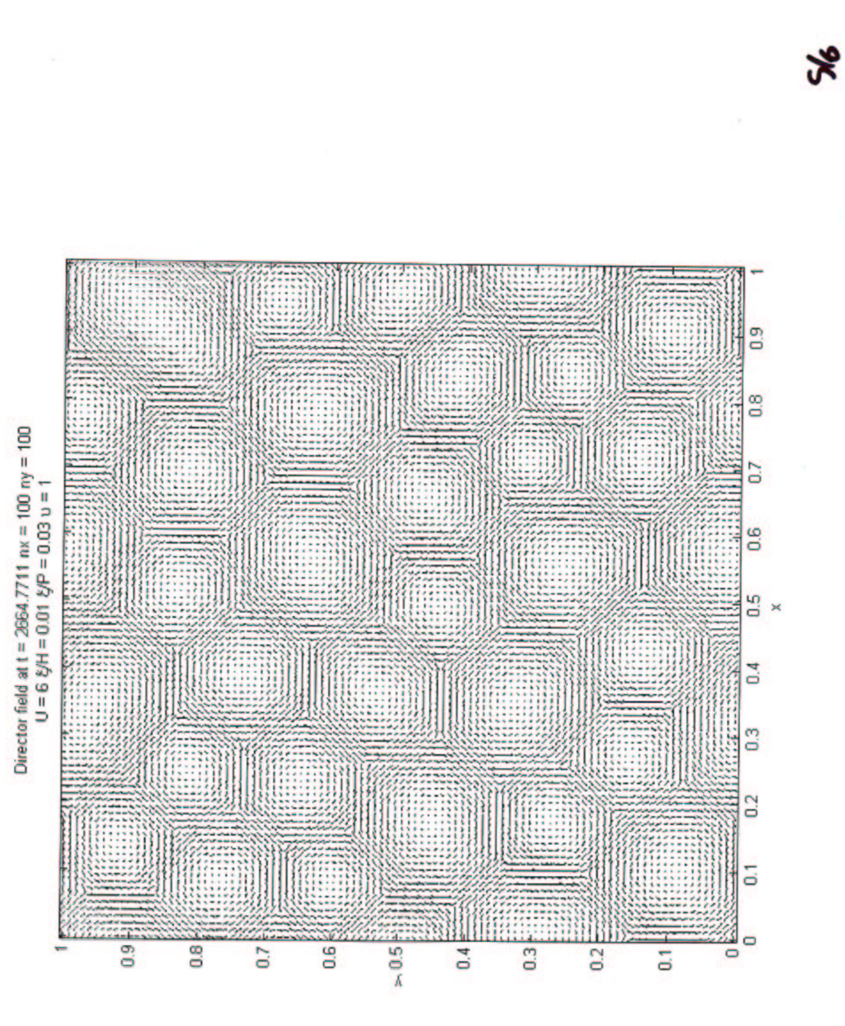
5/6
Director field at t = 2664.7711 nx = 100 ny = 100
U = 6 ξ/H = 0.01 ξ/P = 0.03 u = 1
x
y

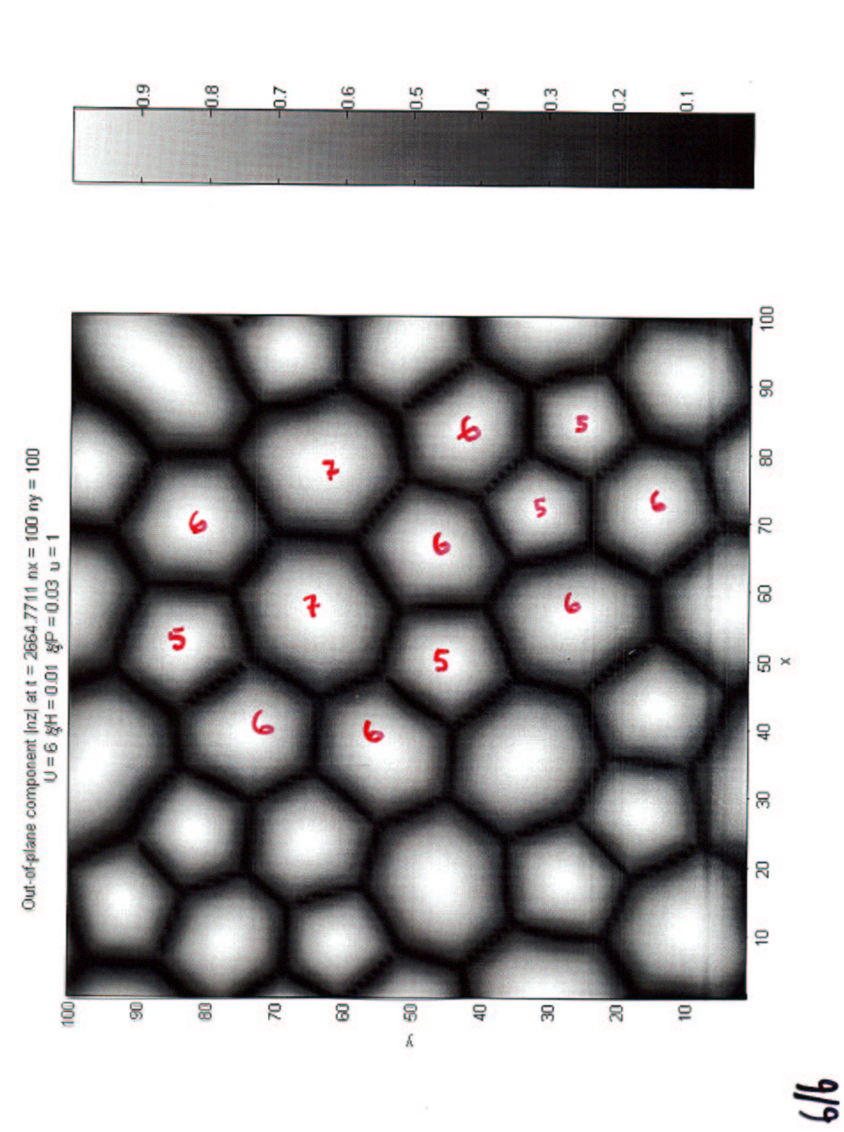
6/6
Out-of-plane component |nz| at t = 2664.7711 nx = 100 ny = 100
U = 6 ξ/H = 0.01 ξ/P = 0.03 u = 1
x
y
5
6
7

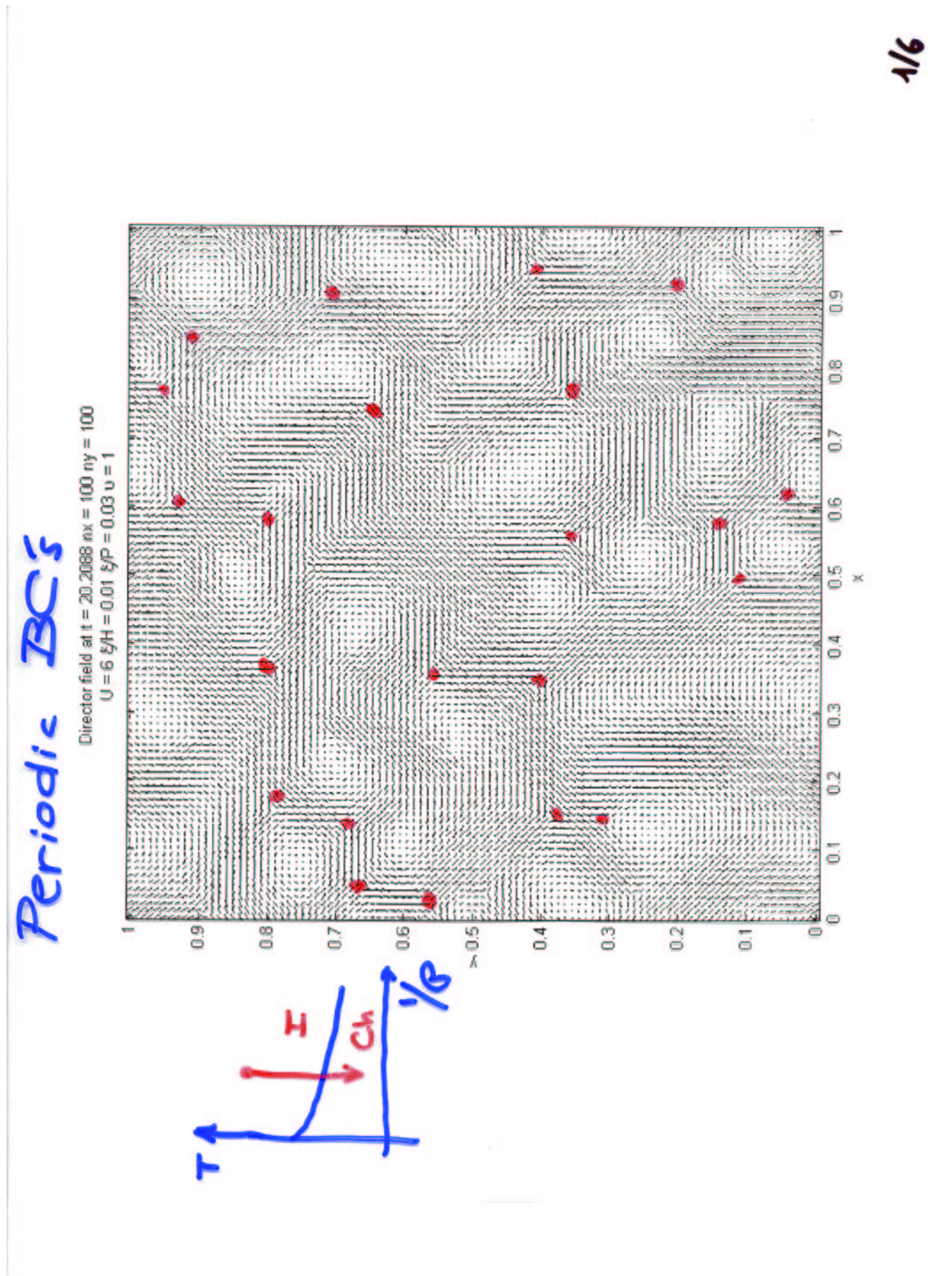

Periodic BC's
Director field at t = 20.2088 nx = 100 ny = 100
U = 6 ξ/H = 0.01 ξ/P = 0.03 u = 1
1/6

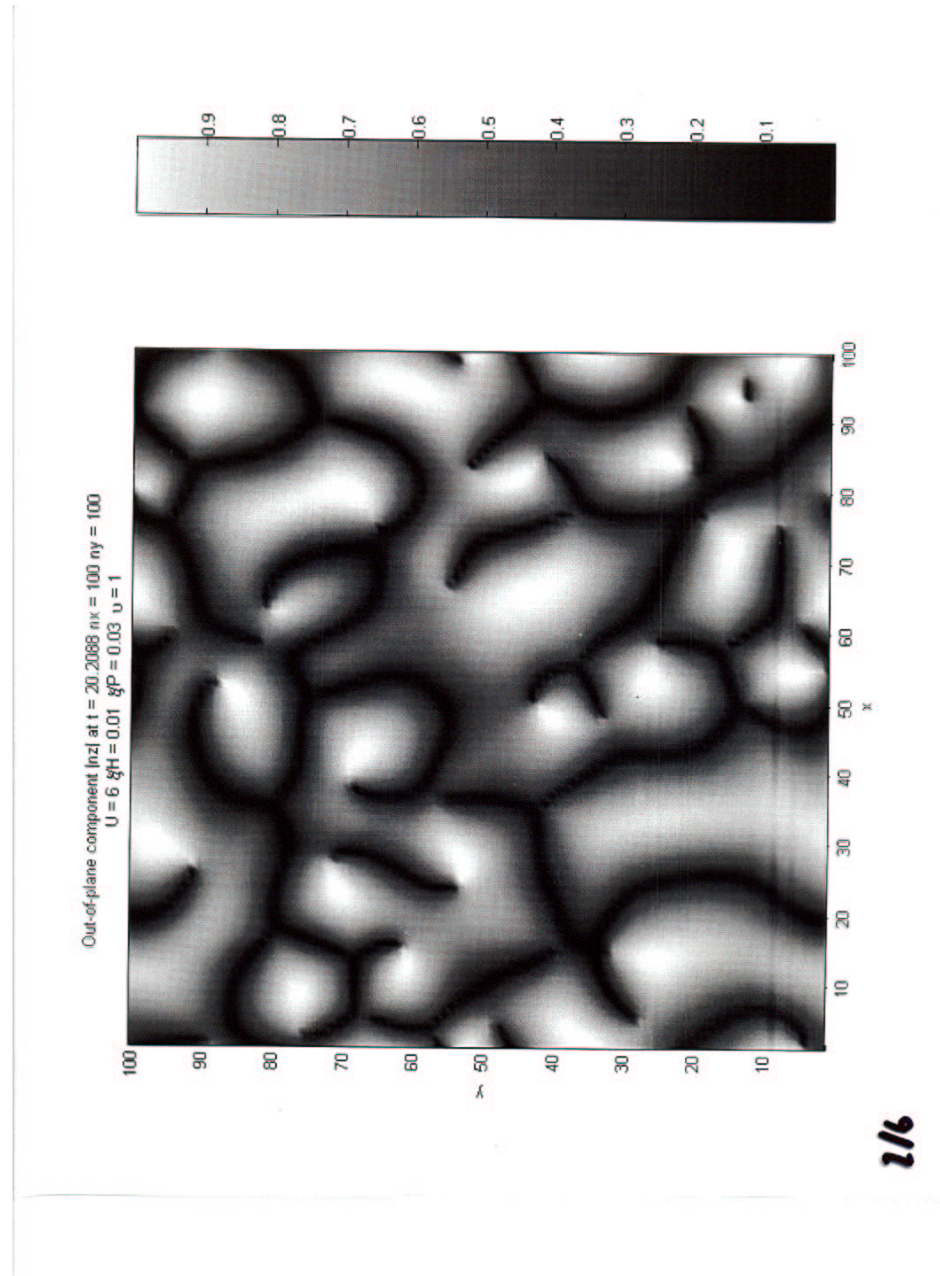

Out-of-plane component |nz| at t = 20.2088 nx = 100 ny = 100
U = 6 ξ/H = 0.01 ξ/P = 0.03 u = 1
2/6

Out-of-plane component of the director $|\mathbf{n}_z|$

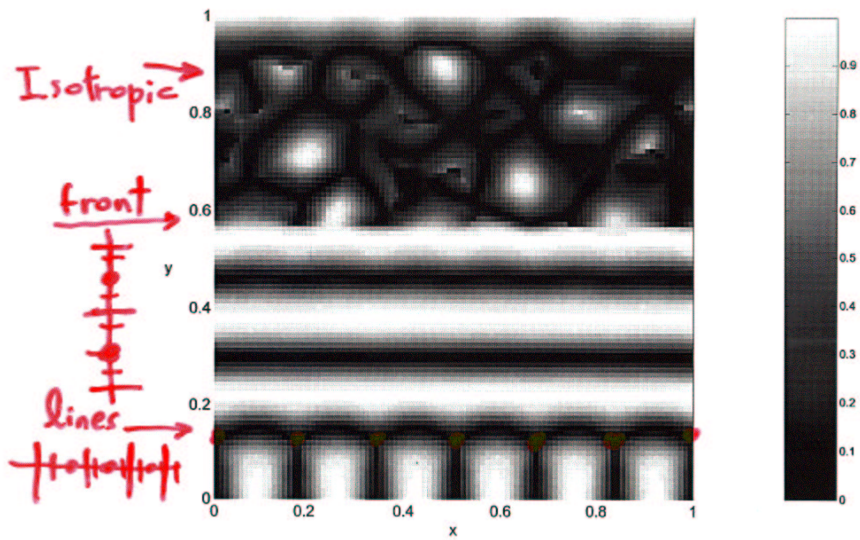

The periodic extinction of light shows the reorientation of the helix axis parallel to the front

36

Uniaxial order parameter front

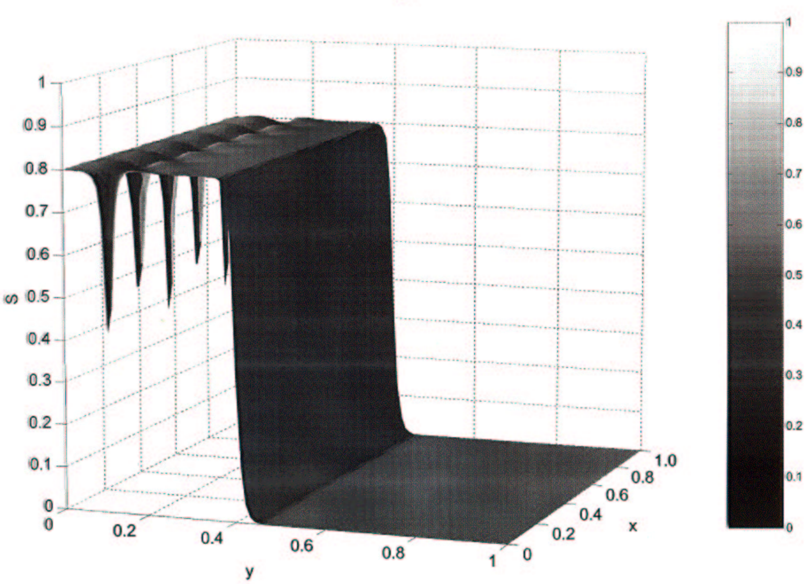

Uniaxial order parameter exhibiting a detachment of disclinations behind the advancing front

34

Carbonaceous Mesophases:

Anistropic Visco-Elastic Textured

Materials

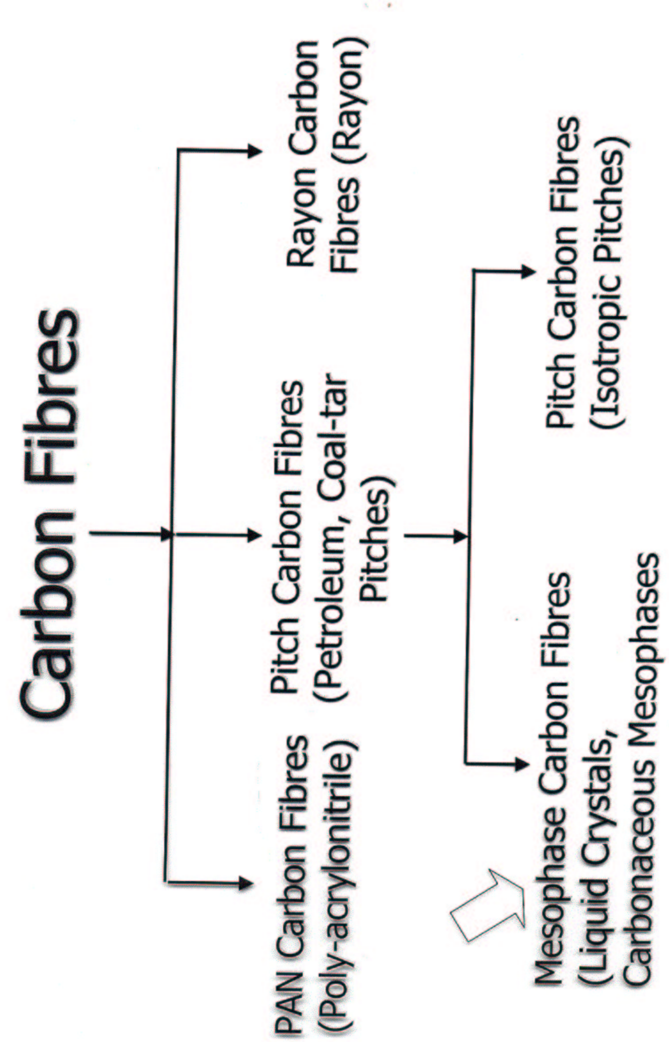

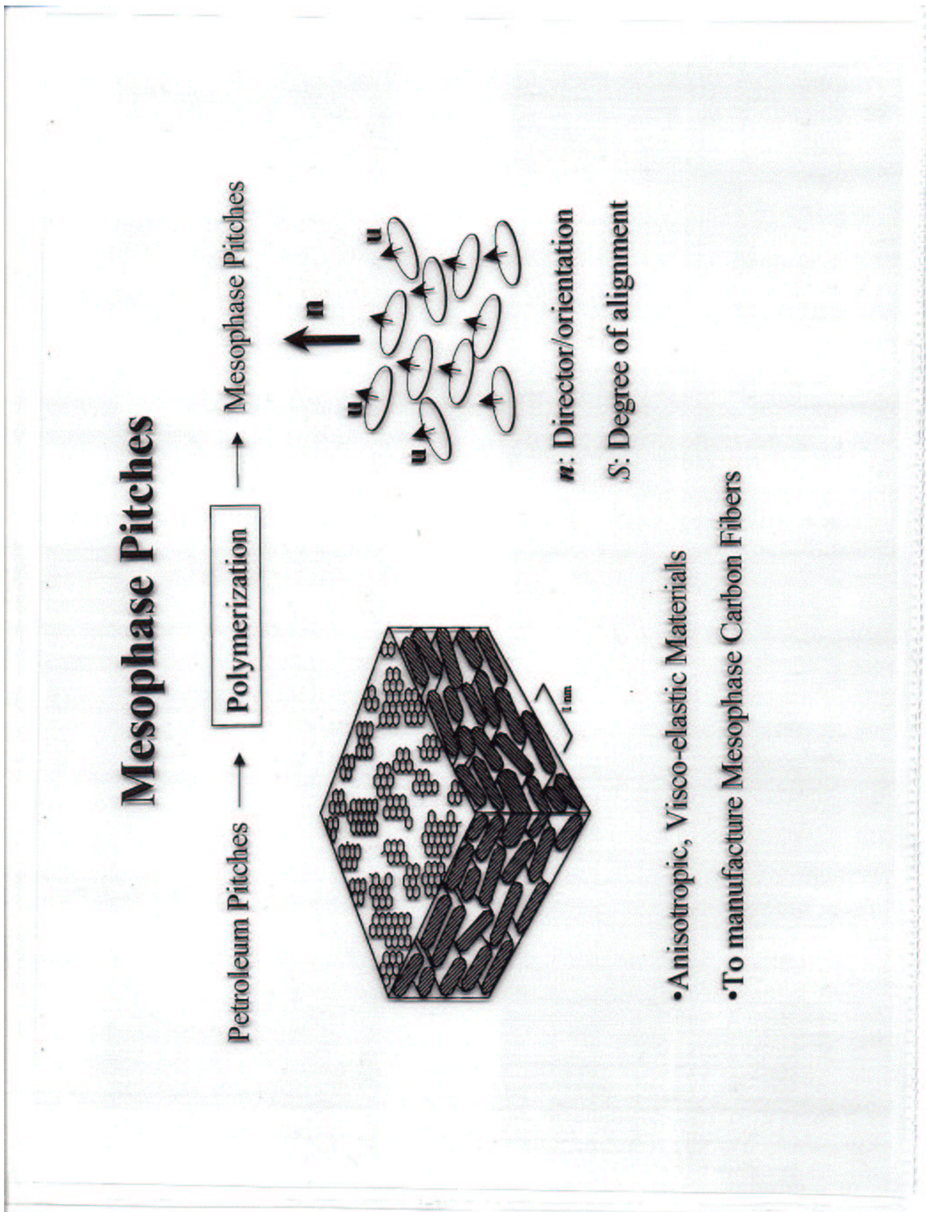

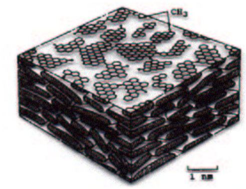

Figure Schematic model of the carbonaceous mesophase, a discotic nematic liquid crystal. From Zimmer and White,[10] reprinted with permission from Academic Press.

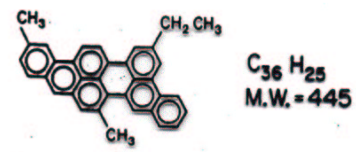

Figure Structure of the "average" molecule, $C_{36}H_{25}$ in a petroleum-derived pitch (Dickinson, ref. 38).

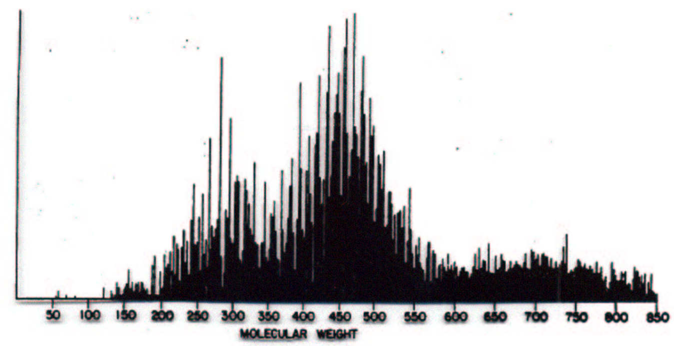

Figure Mass spectrogram of a petroleum-derived pitch (Lewis, ref. 39).

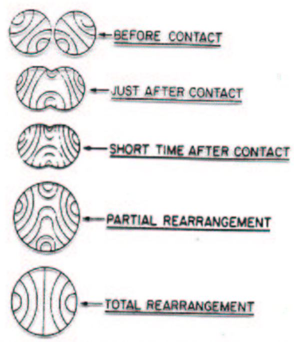

Schematic drawing depicting the collision, coalescence, and rearrangement of mesophase spheres during thermal treatment of a pitch (Singer, Fuel 60, 839, 1981, reprinted with permission from the publishers, Butterworth-Heinemann Ltd.)

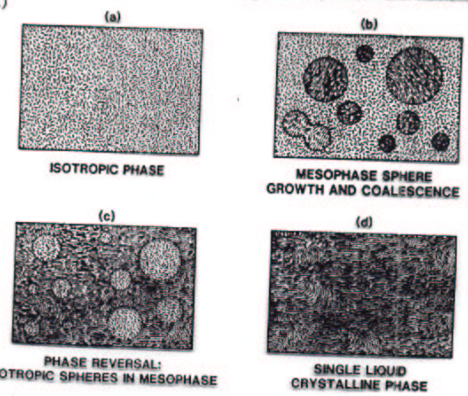

Mesophase development and phase reversal during thermal treatment of a pitch.

CONTINUUM THEORY OF ELASTICITY OF LIQUID CRYSTALS (BY FRANK & OSEEN)

$$2\,Wd = K_{11}\left(\nabla\cdot\mathbf{n}\right)^2 + K_{22}\left(\mathbf{n}\cdot\nabla\times\mathbf{n}\right)^2 + K_{33}\left(\mathbf{n}\times\nabla\times\mathbf{n}\right)^2$$

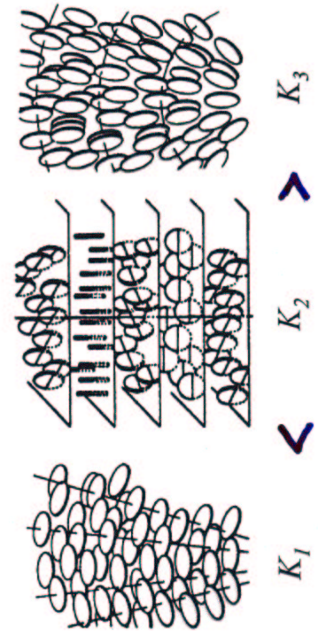

TABLE I
INTERACTIONS BETWEEN WEDGE DISCLINATIONS

$S = +1$	+	$S = -\frac{1}{2}$	⇌	$S = +\frac{1}{2}$
$S = -1$	+	$S = +\frac{1}{2}$	⇌	$S = -\frac{1}{2}$
$S = +\frac{1}{2}$	+	$S = -\frac{1}{2}$	⇌	0
$S = +1$	+	$S = -1$	⇌	0
$S = +\frac{1}{2}$	+	$S = +\frac{1}{2}$	⇌	$S = +1$
$S = -\frac{1}{2}$	+	$S = -\frac{1}{2}$	⇌	$S = -1$

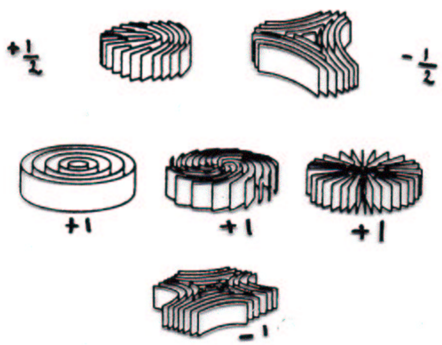

Zimmer & White
Adv. LC, 1982

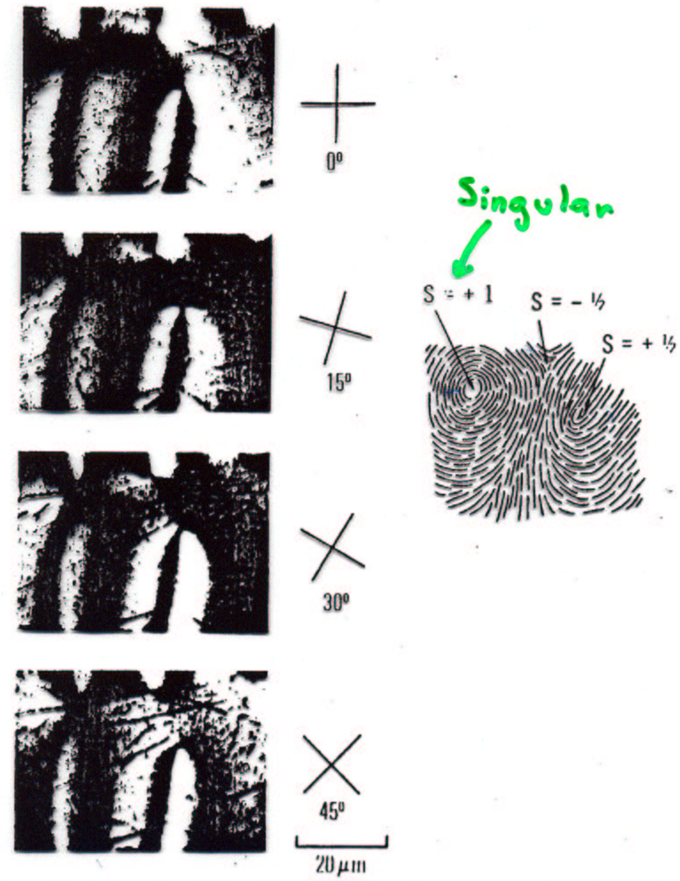

Fig. 25. Configuration of $S = +\frac{1}{2}$ wedge disclination (corotating node), along with $S = -\frac{1}{2}$ and $S = +1$ wedge disclinations, by optical mapping technique.

SPINLINE FOR MESOPHASE PITCH

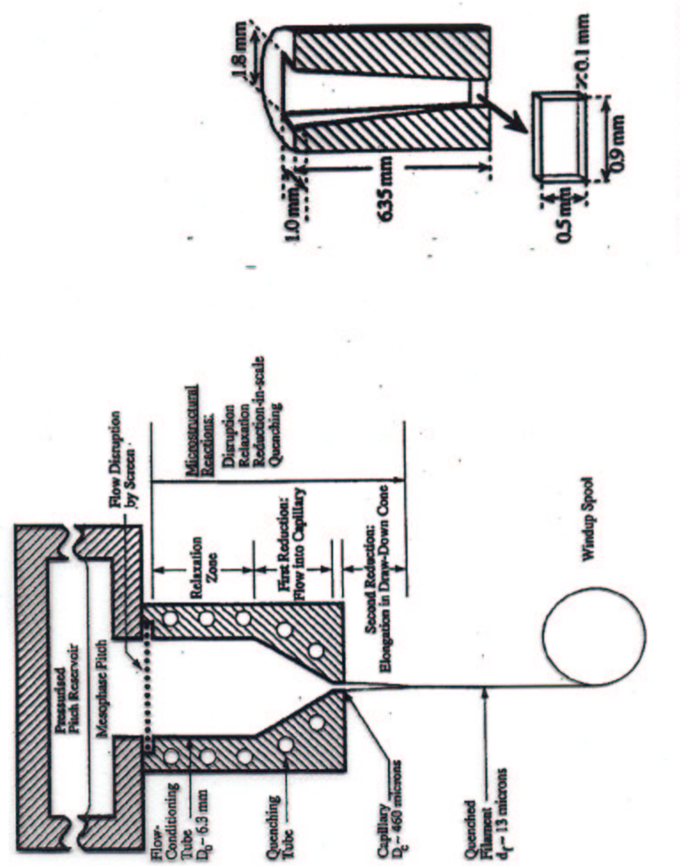

Edie, Clemson University

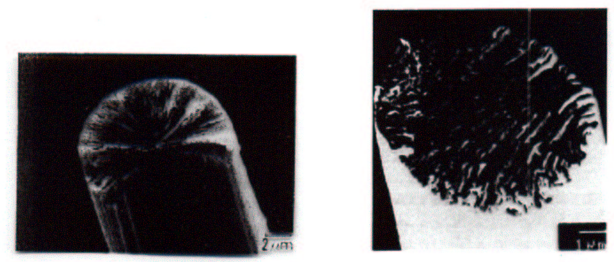

(a) (b)

Ref. Peebles LH, Carbon Fibers Formation Structures and Properties, CRC Press, 1994

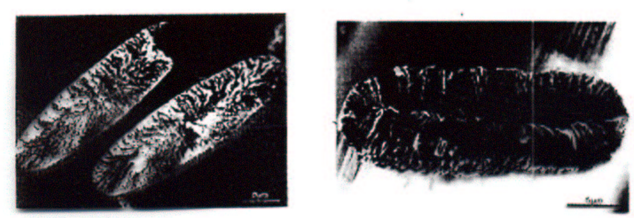

(c) (a)

Ref. Robinson K. E. and Edie D. D., 1996, *Carbon*, **34**(1), 13.

Melt Spinning of Carbonaceous Mesophases

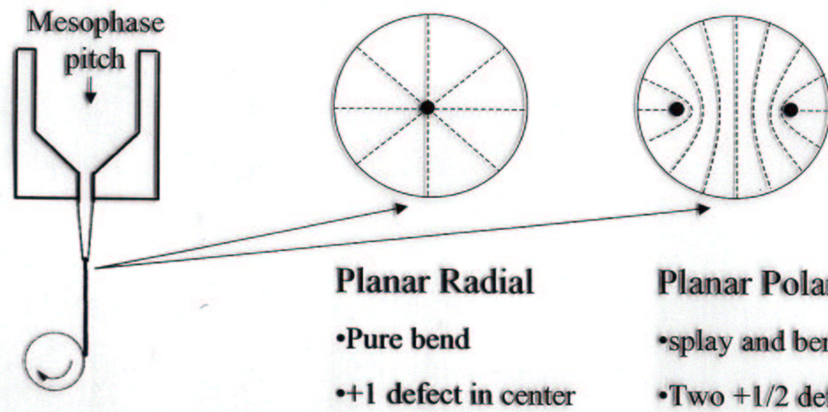

Planar Radial

- Pure bend
- +1 defect in center
- Perpendicular at the boundary
- High temperature

Planar Polar

- splay and bend
- Two +1/2 defects
- Perpendicular at the boundary
- Low temperature

Phase diagram in terms of temperature and dimensionless fiber radius

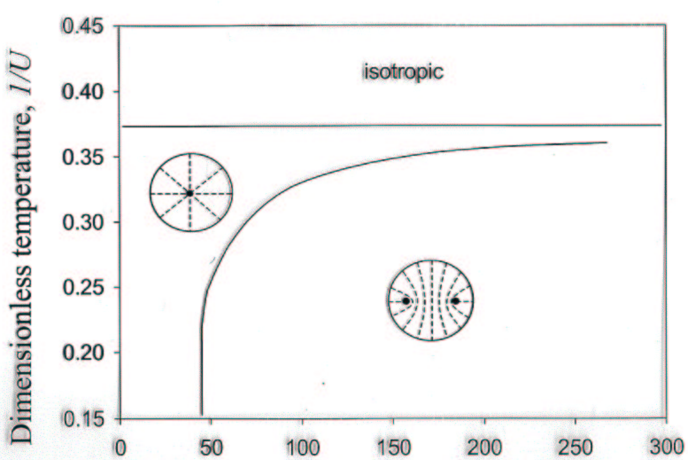

Parameters:

$\tilde{L}_2 = -0.5$

$\tilde{L}_3 = 0$

Dimensionless fiber radius, $\mathcal{R} = \frac{R}{\xi}$

$$\frac{-1}{\frac{1}{U} - \frac{3}{8}} = \left(\mathcal{R} - \mathcal{R}_c\right)^n ;\ n = 0.65, \mathcal{R}_c = 37$$

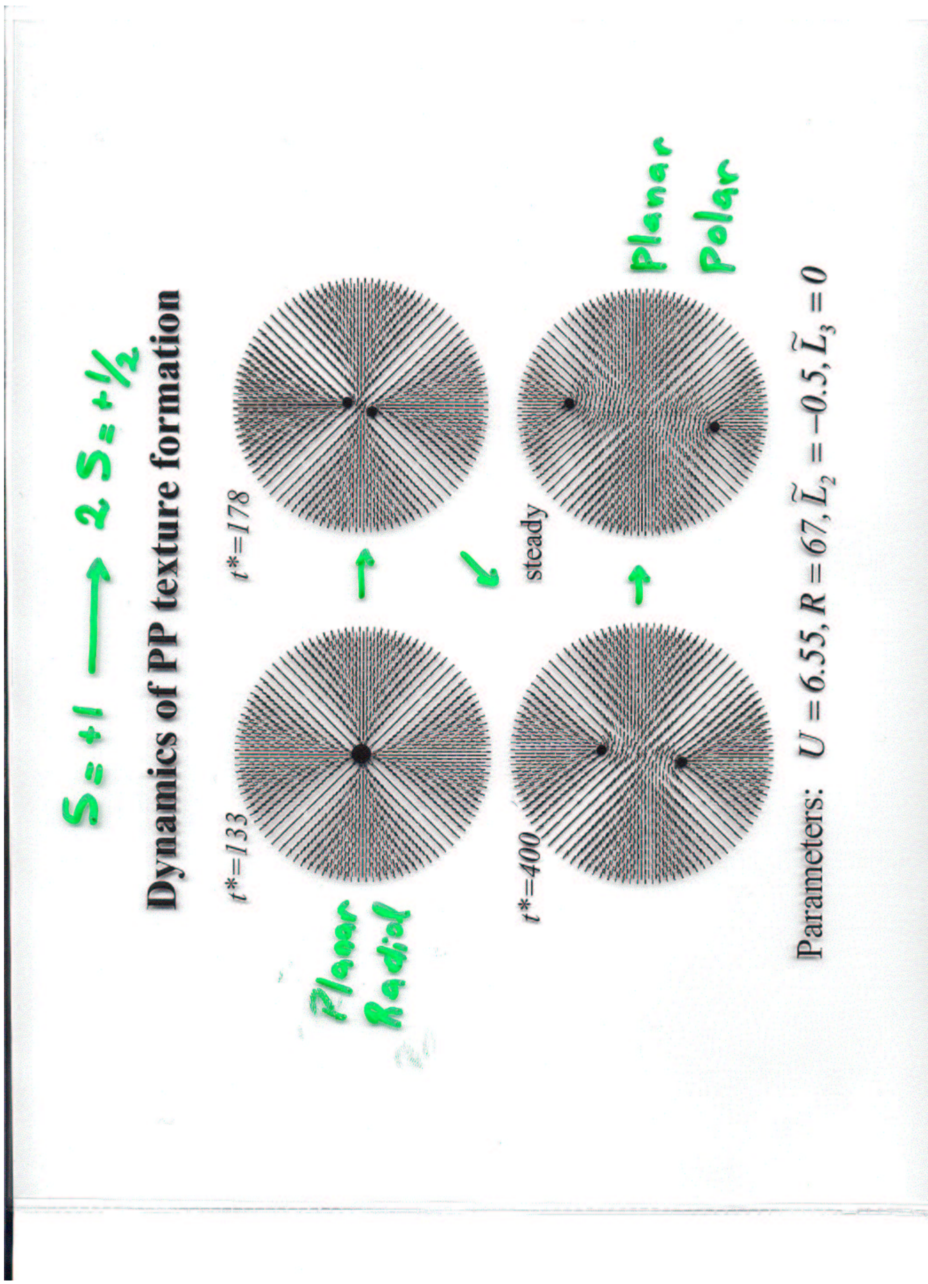

S=+1 ⟶ 2 S=+1/2
Dynamics of PP texture formation
t*=133
t*=178
steady
t*=400
Planar Radial
Planar Polar
Parameters: $U = 6.55, R = 67, \tilde{L}_2 = -0.5, \tilde{L}_3 = 0$

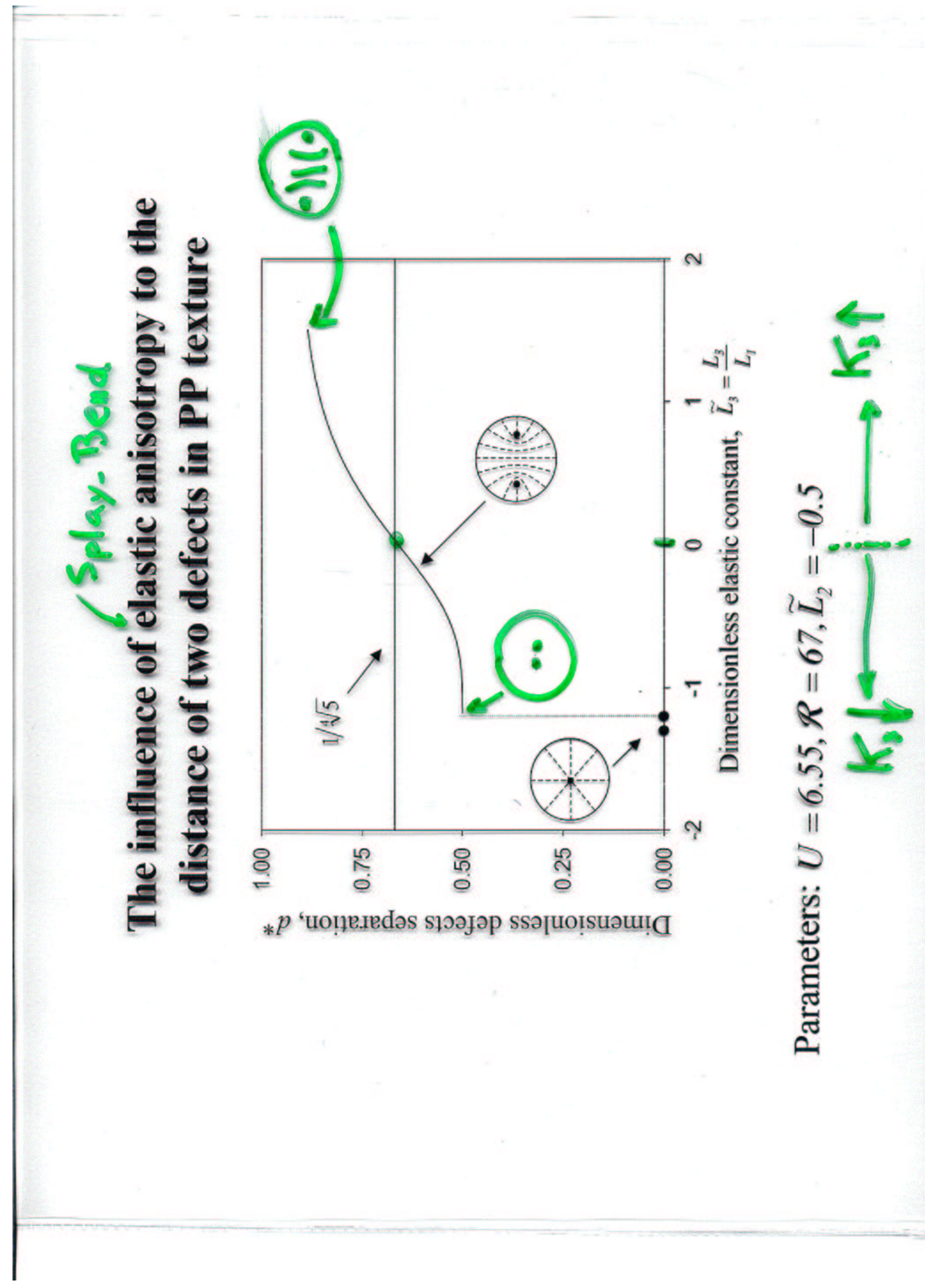

Splay-Bend
The influence of elastic anisotropy to the distance of two defects in PP texture
Dimensionless defects separation, d^*
1.00
0.75
0.50
0.25
0.00
-2
-1
0
1
2
$1/4\sqrt{5}$
Dimensionless elastic constant, $\tilde{L}_3 = \frac{L_3}{L_1}$
Parameters: $U = 6.55, \mathcal{R} = 67, \tilde{L}_2 = -0.5$
K_1
K_3

The distance between two defects of PP texture got from geometric analysis

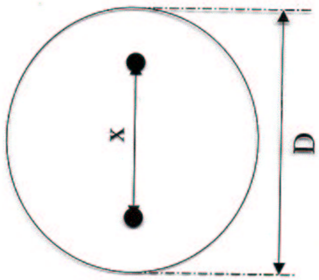

$$x = \frac{1}{\sqrt[4]{5}} D$$

$L_3 = 0 \quad K_1 = K_3$

x: defects separation distance, *D*: fiber radius.

FORMATION OF RIBBON RADIAL: GEOMETRIC EFFECT

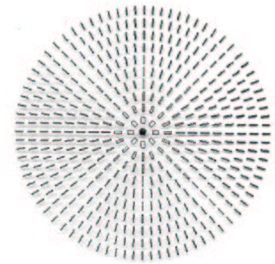

(a)

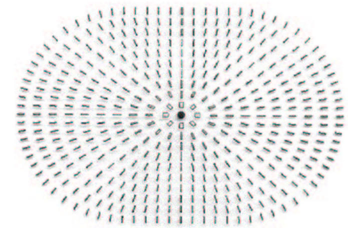

(b)

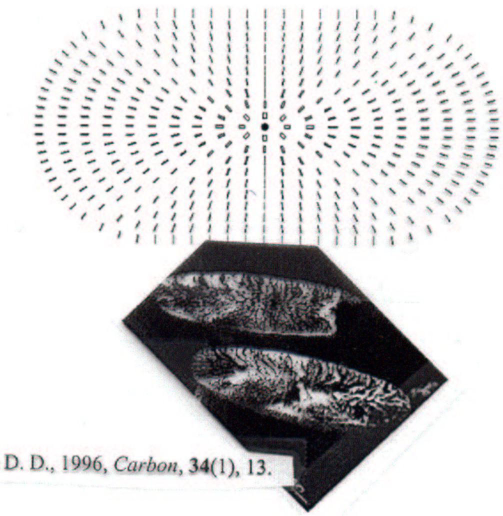

(c)

Robinson K. E. and Edie D. D., 1996, *Carbon*, **34**(1), 13.

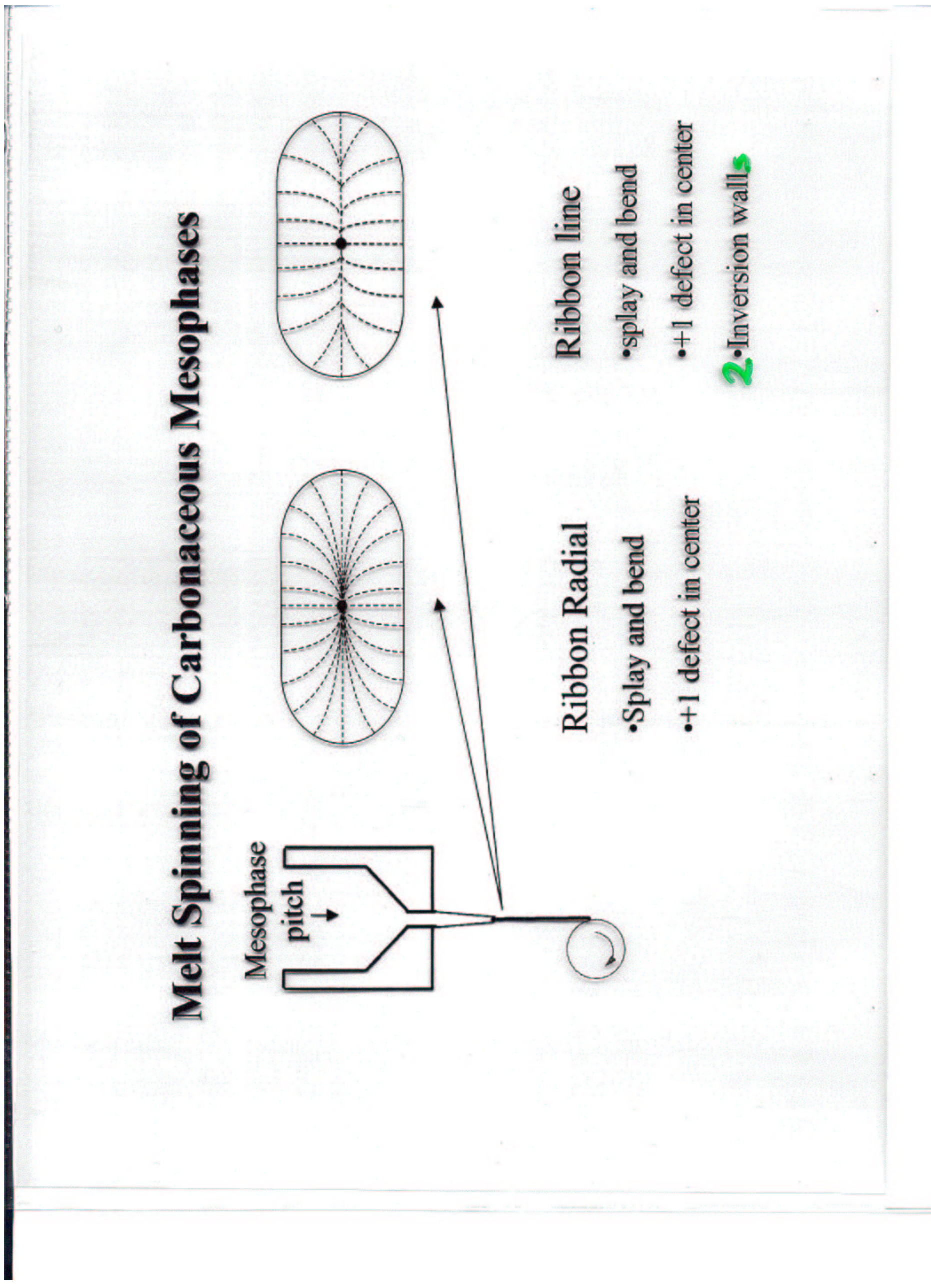
Melt Spinning of Carbonaceous Mesophases
Mesophase pitch
Ribbon Radial
•Splay and bend
•+1 defect in center
Ribbon line
•splay and bend
•+1 defect in center
2•Inversion walls

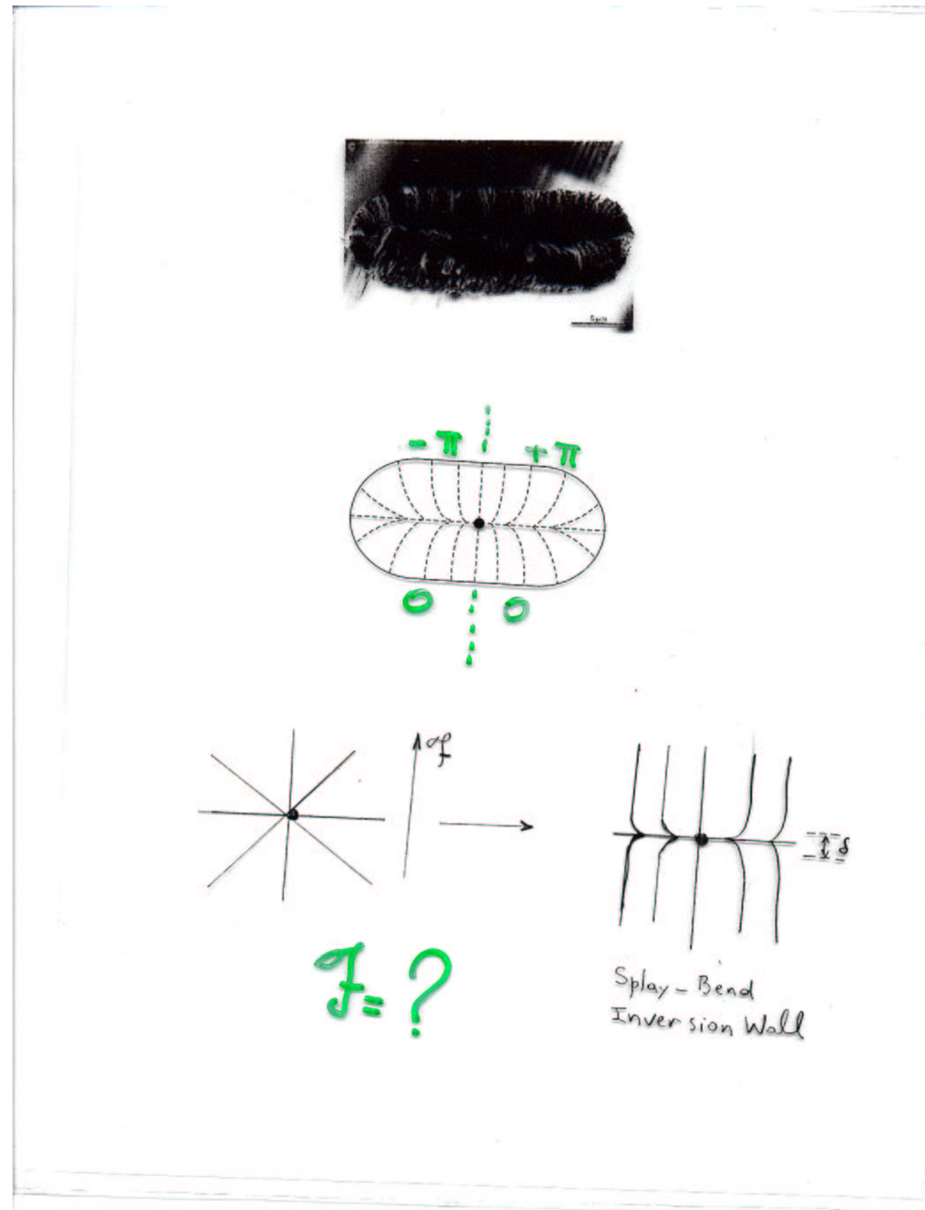
-π
+π
0
0
δ
F= ?
Splay - Bend
Inversion Wall

FORMATION OF RIBBON LINE PLANAR EXTENSIONAL FLOW

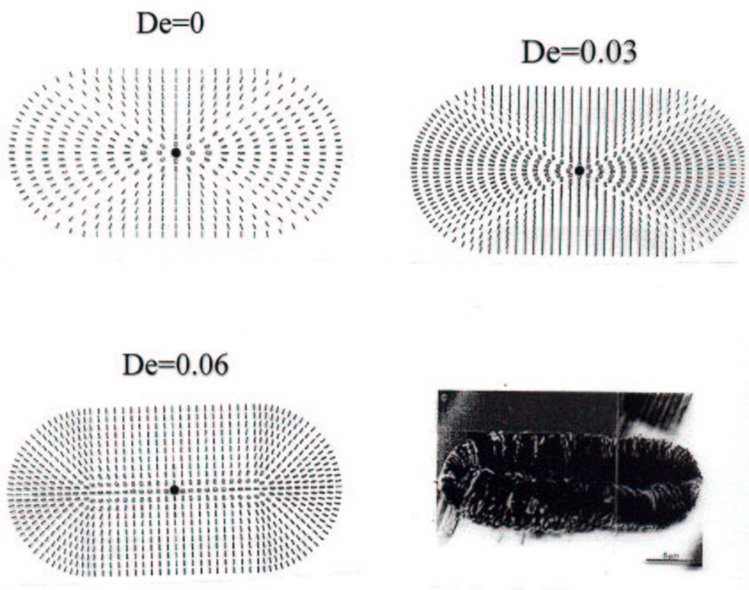

Edie, Carbon 34, 96

Simulation of Flow-Induced Textural Transformations

(I) Isotropic ---> Nematic Phase Transition:

(b) defect nucleation and coarsening
(b) effect of shear on nucleation and coarsening

(II) Defect Nucleation Mechanisms under shear

(c) surface nucleation
(d) bulk nucleation

Formation of Splay-Bend Inversion Wall

Assume:

$$\mathbf{Q} = S_{eq}(\mathbf{nn} - \mathbf{I}/3),\ L_3{=}0,\ \partial\mathbf{Q}/\partial t^* = 0 : \mathbf{n}(y^*) = (\cos\theta, \sin\theta, 0),$$

planar elongational flow:

$$\mathbf{A} = \dot{\varepsilon}\ \widetilde{\mathbf{A}}; \qquad \widetilde{\mathbf{A}} = \begin{bmatrix} -1 & 0 & 0 \\ 0 & 0 & 0 \\ 0 & 0 & 1 \end{bmatrix}$$

Torque Balance Equation:

$$\frac{d^2\theta}{dy^{*2}} + E_e \sin\theta \cos\theta = 0;$$

$$E_e = \frac{\gamma_2 \dot{\varepsilon} R_y^2}{K}; \gamma_2 = -\frac{2\beta\eta S_{eq}}{3}\left(2 + S_{eq} - \frac{S_{eq}^2}{2}\right); \quad K = (L_2 + 2L_1)S_{eq}^2$$

$$E_e = D_e^{\cdot} \left(\frac{R}{\xi}\right)^2 \left\{ S_{eq}\left(2 + S_{eq} - \frac{S_{eq}^2}{2}\right)\left[\frac{1}{(\widetilde{L}_2 + 2)}\right]\right\}$$

$$\tan\left(\frac{\theta}{2}\right) = \exp\left(-y^* \sqrt{E_e}\right)$$

Inversion Wall Thickness : $d^* = \frac{2}{\sqrt{E_e}}$